

Transmembrane protein I6A/anoctamin I inhibitor TI6A_{inh}-A0I reversed monocrotaline-induced rat pulmonary arterial hypertension

Jianye Xie^{1,*} , Wenyuan Liu^{2,*}, Wenjing Lv¹, Xiaohua Han³, Qingnuan Kong⁴, Yuhui Wu^{1,5}, Xin Liu¹, Ying Han¹, Chunying Shi⁶ and Xiujian Jia¹

¹Department of Geriatrics, the Affiliated Hospital of Qingdao University, Qingdao, China; ²Department of General Medicine, the First Affiliated Hospital of Xinxiang Medical University, Xinxiang, China; ³Department of Physiology and Pathophysiology, College of Medicine, Qingdao University, Qingdao, China; ⁴Department of Pathology, Qingdao Municipal Hospital, Qingdao, China; ⁵Department of Cardiology, the Affiliated Cardiovascular Hospital of Qingdao University, Qingdao, China; ⁶Department of Human Anatomy, Histology and Embryology, College of Medicine, Qingdao University, Qingdao, China

Abstract

Transmembrane protein I6A was involved in the development of the monocrotaline-induced pulmonary arterial hypertension model through ERK1/2 activation, and it was considered as potential target for pulmonary arterial hypertension treatment. A pulmonary arterial hypertension rat model was established by intraperitoneal administration of monocrotaline. Noninvasive pulsed-wave Doppler and histological analysis was performed, and it revealed proliferation and remodeling of pulmonary arterioles and right ventricle hypertrophy. In addition, transmembrane protein I6A, proliferating cell nuclear antigen—a proliferate marker, P-ERK1/2 increased following monocrotaline treatment. Expression of transmembrane protein I6A in the pulmonary arteries was co-localized with a specific marker of vascular smooth muscle α -actin. Then, a specific inhibitor of transmembrane protein I6A-TI6A_{inh}-A0I was administered to pulmonary arterial hypertension rats. It was found to alleviate the remodeling of pulmonary arterioles and right ventricle hypertrophy significantly, and decrease the upregulation of proliferating cell nuclear antigen in monocrotaline-induced pulmonary arteries. In addition, TI6A_{inh}-A0I could inhibit the activation of ERK1/2 in pulmonary arterial hypertension model. Transmembrane protein I6A mediated the proliferation and remodeling of pulmonary arterioles in the monocrotaline-induced pulmonary arterial hypertension model. ERK1/2 pathway is one of downstream factors. Long-term use of TI6A_{inh}-A0I in vivo could alleviate remodeling and pressure in pulmonary arterial hypertension.

Keywords

pulmonary arterial hypertension, transmembrane protein I6A, Ca²⁺-activated Cl⁻ channel, vascular remodeling, cell proliferation

Date received: 23 February 2020; accepted: 6 July 2020

Pulmonary Circulation 2020; 10(4) 1–11

DOI: 10.1177/2045894020946670

Introduction

Pulmonary arterial hypertension (PAH) is a common life-threatening cardiopulmonary disease that is usually secondary to lung diseases, such as chronic bronchitis. In its early stage, it is characterized by pulmonary vasoconstriction, pulmonary artery (PA) intimal hyperplasia, proliferation and hypertrophy of pulmonary arterial smooth muscle cells (PASMCs), in situ thrombosis, and an increased extracellular matrix. In its late stage, pathophysiological changes lead to wall thickening and stenosis of the PA and,

*These authors equally contributed to this work.

Corresponding authors:

Jianye Xie, Department of Geriatrics, the Affiliated Hospital of Qingdao University, Qingdao, China.

Email: 1667206728@qq.com

Chunying Shi, Department of Human Anatomy, Histology and Embryology, College of Medicine, Qingdao University, Qingdao, China.

Email: schy1116@163.com

Xiujian Jia, Department of Geriatrics, the Affiliated Hospital of Qingdao University, Qingdao, China.

Email: jiaxiujian2012@163.com



Creative Commons Non Commercial CC BY-NC: This article is distributed under the terms of the Creative Commons Attribution-NonCommercial 4.0 License (<http://creativecommons.org/licenses/by-nc/4.0/>) which permits non-commercial use, reproduction and distribution of the work without further permission provided the original work is attributed as specified on the SAGE and Open Access pages (<https://us.sagepub.com/en-us/nam/open-access-at-sage>).

© The Author(s) 2020.
Article reuse guidelines:
sagepub.com/journals-permissions
journals.sagepub.com/home/pul



subsequently, PAH. This in turn leads to right ventricular failure and death.¹

Pulmonary circulation is a low pressure, low resistance, high flow system. The low resting vascular tone is maintained by the concerted action of ion channels. Depolarization of PASMC and subsequent Ca^{2+} influx are essential for acute vasoconstriction. Currently, L-type voltage-gated Ca^{2+} channels (VGCC) blockers are the only drugs used for the treatment of PH that act directly on an ion channel. Blockade of Ca^{2+} influx by nifedipine, diltiazem, or amlodipine may inhibit excessive vasoconstriction; however, VGCC blockers are only effective in a small subgroup of PAH. Finding new means of depolarization/ Ca^{2+} influx block is still necessary.²

Chloride channels are the main anion channels on the membrane of PASMC, and calcium-activated chloride channels (CaCCs) are the class of outward rectifier, depolarizing Cl^- current, and elevating intracellular Ca^{2+} .² CaCCs are required for normal electrolyte and fluid secretion, transepithelial secretion, cardiac excitation, and neuronal and smooth muscle excitability,^{3,4} and play important roles in the migration and proliferation of PASMCs.^{5,6} The maximal CaCC current decreased in early S phase, and CaCC inhibition attenuated cell growth.⁷ Niflumic acid, which inhibits CaCC currents, weakened the pulmonary arterial tension and vessel remodeling and attenuated PAH in vivo.⁷

Since transmembrane protein 16A (TMEM16A, which we also call anoctamin 1 (ANO1)) was identified as an endogenous CaCC channel protein, it is expressed in various secretory epithelia, the retina, and sensory neurons.⁴ An excitatory Cl^- current provided by TMEM16A is critical for mediating the pressure-sensitive contractile response.⁸ The protein level and activity of cellular TMEM16A positively mediate angiotensin II-dependent vascular remodeling correlating with SMC proliferation.^{4,9} It is also activated in PASMCs of PAH, and increased TMEM16A expression strengthened arteriolar contraction and increased the pressure of pulmonary arteries,¹⁰ it is a possible therapeutic target for PAH.⁴

Drugs acting on TMEM16A have been reported to increase in Cl^- transport, inhibit cell proliferation, induce vasodilation, and prevent vascular remodeling. MONNA, T16A_{inh}-A01, and Ani9 attenuated 5-HT-induced coronary contractions and increased coronary flow.¹¹ Chronic application of benzbromarone significantly decreased right ventricular pressure and reversed remodeling of established PH.¹⁰ Among those inhibitors, T16A_{inh}-A01 can relieve contraction of conduit and intralobar PA from monocrotaline (MCT)-treated rats in a single dose⁴ and can cause a dose-dependent vasodilation response in isolated mesenteric arteries of spontaneously hypertensive rats.¹¹ Besides, T16A_{inh}-A01 could inhibit the proliferation of portal vein SMCs in vitro.¹² These results made us wonder if long-term application of T16A_{inh}-A01 could reverse vascular remodeling by inhibiting SMC proliferation in MCT-induced PAH rats.

In this study, a rat PAH model was established with MCT. Then we measured the pressure change of PA by ultrasonic spectrum analysis and quantified the PA remodeling over time. We also measured the protein levels and location of TMEM16A, and reflected proliferation by proliferating cell nuclear antigen (PCNA) over time. Combined with above results, we choose a time-point when vessel pressure, PA remodeling, and TMEM16A expression reached a plateau, then applied T16A_{inh}-A01 for a period, and reassessed the pressure, remodeling, and proliferation of PA, and also detected the activation of possible downstream ERK1/2 pathway. This study added new data about long-term application of T16A_{inh}-A01 in PAH models in vivo, providing new evidence of T16A_{inh}-A01 improvement on PA remodeling.

Materials and methods

Establishment of a rat PAH model

Fifty male Sprague-Dawley rats (Daren Fucheng Animal Husbandry, Qingdao, China) were randomly divided into five groups: one control group and four groups in which rats were treated with MCT for one (MCT-1), two (MCT-2), three (MCT-3), or four weeks (MCT-4). Rats were housed with a regular 12 h light/dark cycle at a controlled temperature ($23 \pm 1^\circ\text{C}$) and were given free access to food and water. They were sacrificed with CO_2 after ultrasound Doppler experiments.

To establish the PAH model, rats were intraperitoneally injected with 50 mg/kg (body weight) MCT dissolved in 1% DMSO and then observed for occurrence of PAH for up to four weeks, depending on the group. Control animals received 1% DMSO via intraperitoneal injection.

To observe the role of the TMEM16A inhibitor T16A_{inh}-A01 (Sigma, St Louis, USA) in PAH, 30 rats were randomly divided into three groups: DD (DMSO/DMSO), MD (MCT/DMSO), and MT (MCT/T16A_{inh}-A01). Before the experiments with T16A_{inh}-A01, rats in the DD group received 1% DMSO via intraperitoneal injection and rats in the MD and MT groups were intraperitoneally injected with 50 mg/kg (body weight) MCT dissolved in 1% DMSO for a single dose for four weeks. Rats in the DD (negative control) and MD (positive control) groups were injected with 1% DMSO, while rats in the MT group were injected with T16A_{inh}-A01 (0.33 mg/kg to reach $\sim 20 \mu\text{M}$ in plasma) via tail veins every other day for two weeks, the T16A_{inh}-A01 dose referred to Wang's research, and it can induce obvious vasodilation in this dose.⁹

The Guide for the Care and Use of Laboratory Animals (the National Institutes of Health, USA) was followed, and the protocols for animal experiments were approved by the Ethics Committee of the Affiliated Hospital, Qingdao University.

Measurement of pulmonary arterial hemodynamics

The pulmonary arterial hemodynamics of the rat PAH model were noninvasively recorded with a small animal

ultrasound imaging system (Vevo2100, Visualsonics, Canada) to indirectly evaluate PA pressure.¹³ Rats were anesthetized and fixed on the platform of the system. The Doppler probe was positioned beside the sternum at the level of the aortic valve, and pulsed-wave Doppler images of pulmonary arterial blood flow were taken. The sampling volume at the proximal end (5 mm) of the valve leaflets of PA was aligned to maximize the laminar flow and thus to measure pulmonary acceleration time (PAT) and ejection time (ET).⁴ PAT is defined as the interval of time from the initiation of inflow into the PA to the maximal velocity, while ET is the interval of time between the onset and end of pulsed flow velocity in the contraction period. PAT, ET, and the PAT/ET ratio were used for indirect assessment of rats' pulmonary arterial pressure.

Measurement of right ventricular hypertrophy

After the experiments, the rats were anesthetized with 10% chloral hydrate and sacrificed. The heart and lung tissues were quickly retrieved by opening the rats' chests. Residual blood was washed away with PBS solution. The left and right atriums and large vessels were removed from the atrioventricular junction area before the right ventricle (RV) was separated from the left ventricle (LV) and septum (S) by cutting. The separated parts were weighed after the water on them was lightly cleaned with filter paper. The extent of right ventricular hypertrophy was estimated based on the right ventricular hypertrophy index (RVHI) using the following equation: $RVHI = RV/(LV + S)$, where RV, LV, and S are the weights of RV, LV, and S, respectively.

Hematoxylin and eosin (HE) staining and wall thickness (WT) measurement of PA

Right lung tissues were crosscut and fixed in 4% paraformaldehyde for 48 h. Then, the tissues were dehydrated until they looked transparent, impregnated with wax, and sectioned into 6- μ m-thick slices that were affixed to glass slides before baking and staining with HE using an HE staining kit (Beyotime Biotech Inc., Shanghai, China).

Ten random view fields were collected from 10 slices, which were chosen from every five consecutive slices. External diameter (ED) vessels (50–150 μ m) were analyzed using an Image-Pro Plus imaging analysis system, to determine the total area (TA), lumen area (LA), WT, and ED. The ratio (WA%) of wall area ($WA = TA - LA$) to the TA of a cross-sectioned pulmonary arteriole was determined using the following formula: $WA\% = (TA - LA)/TA \times 100\%$. The ratio (WT%) of WT to ED was derived using the following formula: $WT\% = (2 \times WT/ED) \times 100\%$.

Western blotting

Isolation of PA. Small PAs were isolated from the rats anesthetized with 10% chloral hydrate. Then, these PAs were

dissected under a stereoscopic microscope with eyelid tweezers and ophthalmic scissors. The arterial fat and fibrous connective tissues were completely stripped off of the PAs until they could be classified as grade 2 or 3 (i.e. small arteries). To remove arterial endothelial cells, the arteries were cut open along the major axis from the outside and the intima was wiped with sterile cotton swabs 4–6 times. The PAs denuded with endothelium after paraformaldehyde fixation was stored at -80°C so they were ready for Western blot, reverse transcription-quantitative polymerase chain reaction (RT-qPCR), and fluorescent immunostaining.

PA tissues were weighed and mixed with protein lysate buffer (CWBIO, Beijing, China) at a ratio of 1:10 (PA tissue weight/protein lysate buffer weight). The buffer was freshly added with PMSF and other phosphatase inhibitors (CWBIO, Beijing, China). The concentrations of proteins were measured using a BCA kit, and 30 μ g of whole-cell proteins was applied to each lane of 10% SDS-polyacrylamide gels. The proteins were separated on the gel and then transferred onto polyvinylidene difluoride membranes, which were blocked with 5% skimmed milk for 2 h and immunoblotted with a primary antibody against TMEM16A (Abcam, Cambridge, UK) at a dilution of 1:1000, a PCNA (Boster, CA, USA) at a dilution of 1:250, or an antibody against β -actin (Santa Cruz Biotechnology, Dallas, TX, US) at a dilution of 1:1000. Immunoblotting was performed in Tris-buffered saline plus 1% Tween-20 (TBST) overnight at 4°C and 1 h at room temperature. The membranes were washed with TBST and incubated with a horseradish peroxidase-conjugated goat anti-rabbit or goat anti-mouse secondary antibody for 2 h at room temperature. Then the membranes were washed and visualized with Pierce ECL (Millipore, MA, USA). The intensity of the target bands was normalized to that of β -actin.

RT-qPCR

Total RNA was extracted from PA tissues (see "Isolation of PA" section) using TRIzol reagent (Invitrogen, CA, USA). Then, a RT-qPCR was performed according to the instructions provided with the PrimeScript-RT reagent kit with a gDNA Eraser (Perfect Real Time) (TaKaRa Bio, Japan). The RT-qPCR conditions for the applied cDNAs were as follows: 1 cycle at 95°C for 3 min, 40 cycles at 95°C for 5 s and 56°C for 30 s, and a melt curve from 65.0 to 95.0°C with a change of 0.5°C every 5 s. Primer sequences used for RT-qPCR was seen in Table 1.

Fluorescent immunostaining of PAs

PAs were isolated as described above for frozen tissue dissection. Slices of artery tissues were incubated overnight with rabbit anti-TMEM16A antibodies and mouse anti-smooth muscle α -actin (SMA) antibodies (Abcam, Cambridge, MA, US). After washing with phosphate-buffered saline, the slices were exposed to Alexa Fluor 488 Affinipure Goat Anti-mouse

IgG and Alexa Fluor 594 AffiniPure Goat Anti-Rabbit IgG for incubation for 1 h. The cellular nuclei in the slices were counterstained with DAPI (ZSGB-BIO, Beijing, China). The fluorescent images were examined with fluorescent inverted microscopy (Nikon, Tokyo, Japan).

Experimental design and data analysis

Experiments were blinded among experiment operators and intervention implementers, including the Western blot, immunofluorescence confocal staining, immunohistochemical staining, and MCH with or without T16Ainh-A01 treatment.

All data were expressed as mean \pm SEM. For Western blot and RT-qPCR, n represents the number of independent experiments performed on different rats. Statistical analysis was determined by an unpaired two-tailed Student's t -test between control group and the MCT-treated group in Figs 1 and 2. One-way analysis of variance followed by least significant difference comparison, with a 95% confidence interval, was performed to detect the significance between groups in Figs 4 and 5.

Results

PA hemodynamics signs of MCT-induced PAH model

To evaluate whether a rat PAH model was successfully established, the parameters PAT and ET, which reflect the time required to open pulmonary arterial valves and PA hemodynamics, as well as the size of right atrium were measured with a small animal ultrasound imaging system. The system provides noninvasive pulsed-wave Doppler images of PA hemodynamics and echocardiographic images of the right atrium.¹³ PET, ET, and the size of the right atrium are measured using the images. These measurements reflect changes in the PA pressure in the rat model. When PA pressure rises, the opening time of PA valves is shortened.

The PA ultrasound hemodynamic images are shown in Fig. 1a. These images were used to determine the values of PAT and ET, which in turn were used to calculate the ratio of PAT to ET. The results statistically showed that PAT, ET, and PAT/ET were significantly decreased in the MCT-3 (three-week model) and MCT-4 (four-week model) groups compared to the levels detected in the control group ($P < 0.05$ and $P < 0.01$, Fig. 1b). This indicates that PA pressure may have significantly increased three weeks after MCT treatment. PAT, ET, and PAT/ET in the MCT-1 (one-week model) and MCT-2 (two-week model) groups did not change significantly compared to the control (Fig. 1b). These results suggest that the rat PAH model was successfully created three weeks after MCT treatment.

Pathological changes in the pulmonary tissues of MCT-treated rats

We also observed the pathological changes that occurred in lung tissues, especially pulmonary arterioles. HE staining

was performed on the lung tissues (Fig. 1c). In contrast to the control, starting in week 2 of MCT treatment, HE-stained pulmonary vessels showed poor continuity between vascular endothelial cells, proliferation and hypertrophy of vascular smooth muscle cells, and thickened vascular walls. The pathological remodeling of vessels became increasingly visible and severe with increasing MCT treatment time; in the MCT-4 group, the vessel lumen was occluded and a large number of inflammatory cells had infiltrated the tissues. Simultaneously, the pathological changes and remodeling were digitized using an imaging analysis system, Image-Pro Plus, and were expressed with the WA and WT of cross-sectioned pulmonary arterioles. As shown in Fig. 1d, both WA% (WA relative to TA of the cross-sectioned vessel) and WT% (WT relative to ED of the vessel) increased significantly from week 2 of MCT treatment (Fig. 1d). Likewise, the RVHI, which reflects the change in the weight of the RV relative to the LV, was significantly increased (Fig. 1d).

Upregulation of TMEM16A, PCNA, and P-ERK1/2 expression in the PAs of PAH

To study whether TMEM16A was involved in the process of MCT-induced PAH formation, we examined the level of protein expression of TMEM16A in PAs isolated from MCT-treated rats. It revealed that TMEM16A mRNA and protein expression were dramatically upregulated starting at week 2 after MCT treatment, and increased during the development of the disease (Fig. 2a, d, and g). In addition, the expression of nuclear protein PCNA, whose expression is proportional to the cell growth rate, also significantly increased, accompanying with the expression of TMEM16A (Fig. 2b and e). It was reported TMEM16A maybe promote the cell proliferation in PA. ERK1/2 signaling pathway mediated the growth effect of TMEM16A in tumor,¹⁴ so we detected P-ERK1/2 levels in PAH model, and found P-ERK1/2 was elevated after two weeks following MCT treatment (Fig. 2c and f).

Localization of TMEM16A proteins in the smooth muscle cells of pulmonary arterioles

The results of fluorescent immunostaining showed that TMEM16A proteins were co-localized with SMA, a cellular protein that was specifically expressed in the smooth muscle cells, which indicated that TMEM16A was endogenously expressed in vascular smooth muscle. In line with the results of Western blotting and RT-qPCR, the TMEM16A signals in smooth muscle cells started to become stronger at week 2 of MCT treatment and were gradually strengthened as the MCT treatment time increased (Fig. 3).

TMEM16A inhibitor T16A_{inh}-A01 improved the PAH of MCT-treated rats

T16Ainh-A01 has been reported to be a TMEM16A-specific inhibitor in various types of tissues. It not only inhibited the

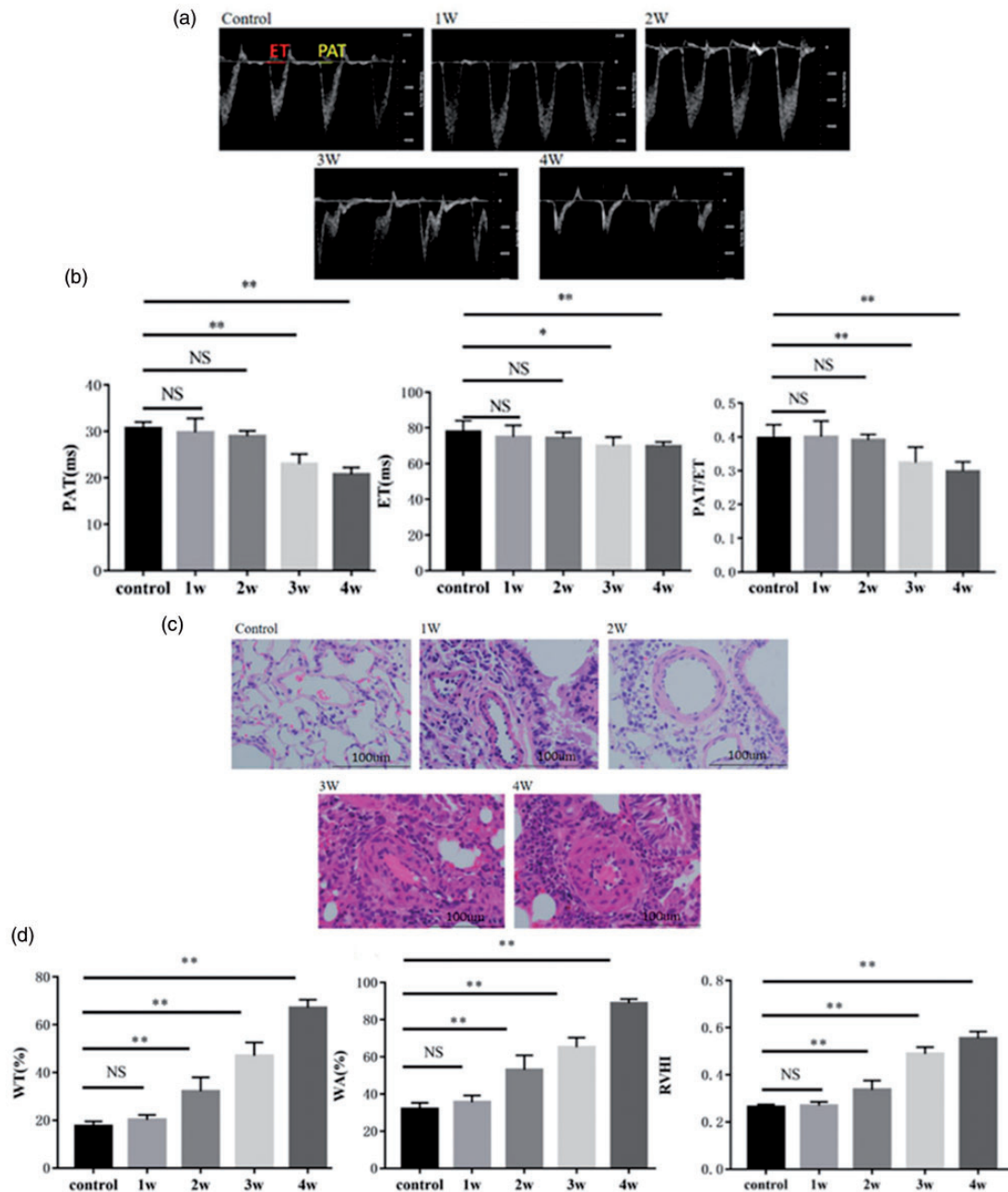


Fig. 1. MCT-induced PAH modeling and related changes. (a) Representative Doppler images of pulmonary arterial outflow recorded from the rats treated with MCT for 0 (control), 1 (1W), 2 (2W), 3 (3W), or 4 weeks (4W). In the control panel, PAT refers to PA acceleration time, while ET refers to ejection time. The value ranges (milliseconds) of each are indicated by the bars. (b) Analytic data for PAT, ET, the PAT/ET ratio. (c) Representative HE-stained slices of pulmonary tissues obtained from rats treated with MCT for 0 (control), 1 (1W), 2 (2W), 3 (3W), or 4 weeks (4W). Arrows indicate the vascular walls. Red blood cells existed inside the lumens of some vessels lined by endothelial cells (blue). Inflammatory cells around cross-sectioned vessels were stained blue. (d) Analytic data regarding WT%, WA% (WT% is the ratio of vascular WT to the ED of the vessel, while WA% is the ratio of vascular wall area to the TA of the cross-sectioned vessel), and the RVHI of rats with MCT-induced PAH. See the “Materials and methods” section for our calculation of the RVHI. Arterioles with an ED of 50–150 μm were selected for measurement using an Image-Pro Plus imaging analysis system. *: $P < 0.05$ versus control; **: $P < 0.01$ versus control. $n = 7-10$ for each group. NS: not significant; RVHI: right ventricular hypertrophy index; WA: wall area; WT: wall thickness.

channel activity of TMEM16A but also suppressed its effect on cellular proliferation. We applied this inhibitor to the rat PAH model and observed its effect on PAH. Although PAT and PAT/ET were dramatically decreased after MCT

treatment (when comparing the DD and MD groups, $P < 0.01$; Fig. 4a and b), they were significantly increased after T16Ainh-A01 treatment when comparing the MD and MT groups ($P < 0.01$). The results indicate (Fig. 4b)

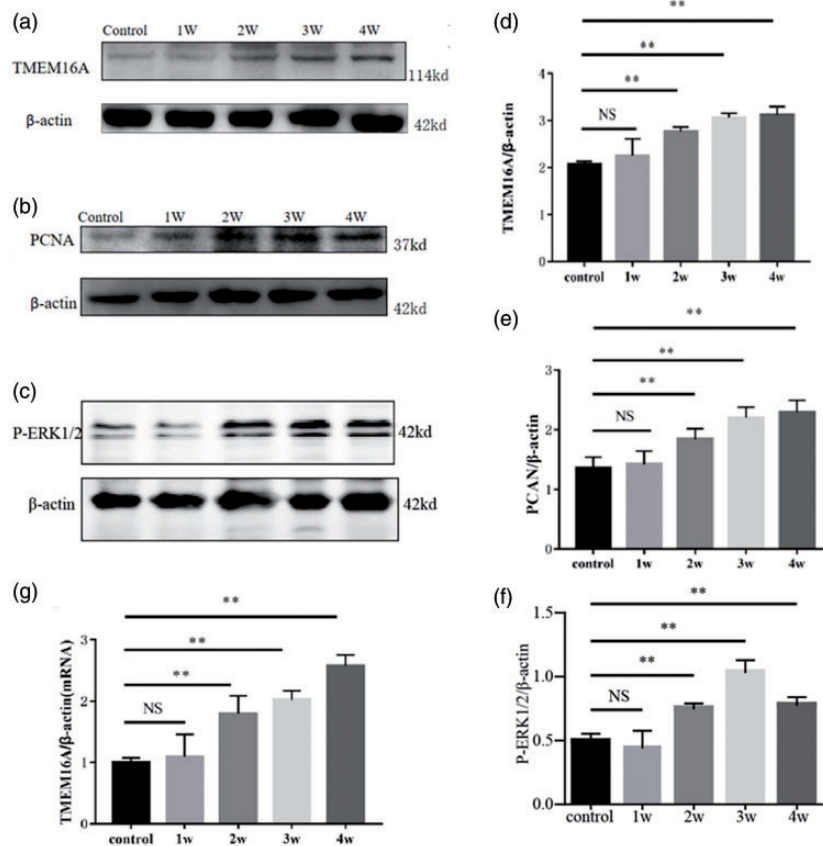


Fig. 2. Upregulation of TMEM16A expression in the PAs of PAH-modeling rats and its correlation with PCNA and WA%. Representative Western blots are shown. Pulmonary arterial tissues were obtained for Western blots from rats treated with MCT for 0 (control), 1 (1W), 2 (2W), 3 (3W), and 4 weeks (4W). Representative Western blot band of TMEM16A (a), PCNA (b), P-ERK1/2 (c) of pulmonary arterial tissues from rats treated with MCT for 0 (control), 1 (1W), 2 (2W), 3 (3W), and 4 weeks (4W). (d) to (f) Analytic data of TMEM16A, PCNA, P-ERK1/2 protein expression. (g) TMEM16A mRNA expression of pulmonary arterial tissues from rats treated with MCT for 0 (control), 1 (1W), 2 (2W), 3 (3W), and 4 weeks (4W). **: $P < 0.01$ versus control. $n = 6$ for each group. ERK1/2: extracellular regulated protein kinases; NS: not significant; PCNA: proliferating cell nuclear antigen; TMEM16A: transmembrane protein 16A.

that the PA pressure was decreased by T16A_{inh}-A01 and that the inhibitor greatly improved PAH. However, it did not lead to complete recovery of PAH; the PAT and PAT/ET ratio were still significantly lower in the MT group than in the DD negative control group ($P < 0.01$). Additionally, the inhibitor did not significantly affect ET when comparing the MD and MT groups. Fig. 4d shows that the values of WT%, WA%, and RVHI were significantly increased at week 4 of MCT treatment when comparing the DD and MD groups. However, consistent with the changes in PAT, WT%, WA%, and RVHI values were significantly reduced by T16A_{inh}-A01 treatment in the MT group compared to those in the MD group. In Fig. 4c, an HE-stained pulmonary arteriole wall was shown to be thickened by MCT treatment (MD panel), while the thickened wall was significantly improved by the inhibitor (MT panel). Despite the significant improvement, there were still differences between DD and MT (Fig. 4c and d), which implied incomplete recovery of pulmonary arteriole remodeling. Overall, the results indicated that the pulmonary vascular remodeling and right ventricular

hypertrophy of PAH rats were partially but significantly improved with use of T16A_{inh}-A01.

ERK1/2 mediated the pro-proliferating effect of TMEM16A activity

We found that the TMEM16A inhibitor T16A_{inh}-A01 weakened nuclear protein PCNA overexpression in the PAs of PAH rats (Fig. 5a and b), indicating that TMEM16A activity had probably enhanced the proliferation of pulmonary arterioles in PAH rats. ERK1/2 is known to mediate some of the cellular roles of TMEM16A,^{14,15} we tested this cellular factor, finding that the inhibitor significantly inhibited phosphorylation of ERK1/2 in the PAs of rats ($P < 0.05$, Fig. 5c and d). In fact, it almost completely inhibited phosphorylation, as comparison between DD and MT did not reveal any significant difference ($P > 0.05$). The results suggested that ERK1/2 is one of the factors downstream of TMEM16A that mediate its pro-proliferating effect on the pulmonary arterioles of PAH rats.

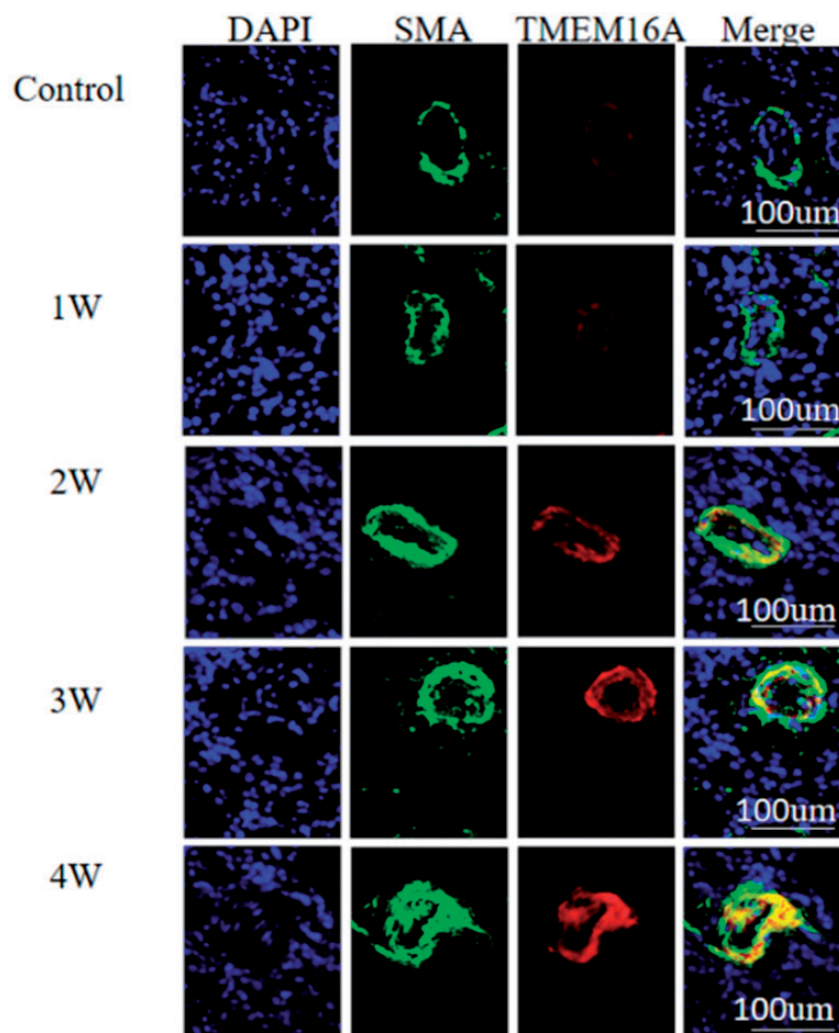


Fig. 3. Localization of TMEM16A in the arterioles of lung tissues from MCT-treated rats. Lung tissues were isolated from rats treated with MCT for 0 (control), 1 (1W), 2 (2W), 3 (3W), and 4 weeks (4W). Nuclei were counterstained with DAPI (blue). SMA (green) indicated the location of vascular smooth muscle cells. TMEM16A was shown by red fluorescence. “Merge” represents merged SMA and TMEM16A signals. DAPI: diamidino-phenyl indole; SMA: smooth muscle α -actin; TMEM16A: transmembrane protein 16A.

Discussion

This study, which was based on successful establishment of a rat PAH model, was the first to apply T16Ainh-A01, a TMEM16A inhibitor, *in vivo* for a long period. It demonstrated that TMEM16A overexpression in PAs probably participated in the process of PAH formation induced by MCT treatment in rats.

An increasing body of evidence points out that proliferation and migration of vascular smooth muscle cells, continuous contraction of pulmonary vessels, and dysfunction of vascular endothelia are the major factors that cooperatively or synergistically lead to vascular remodeling and to the occurrence of PAH. Therefore, various studies have used inhibition of vascular remodeling and proliferation of PSMCs to prevent and treat PAH.

Ultrasonic evaluation of the MCT-induced rat PAH model

PAT, ET, and PAT/ET, reflecting the vascular pressure and blood flow spectrum, began to decrease significantly from three weeks after MCT treatment. However, WT%, WA%, and RVHI, reflecting the vascular smooth muscle cells proliferation and vascular walls remodeling, began to change significantly from two weeks after MCT treatment, a week earlier than the changes of PAT, ET, and PAT/ET. The reason maybe either due to the insensitivity of vascular ultrasound, an indirect method of detecting pressure *in vivo*, or this indicated that pulmonary arterial pressure elevation has some time delay than the vessel wall thickening and remodeling. Therefore, it would be significant to begin to give therapeutic intervention once mild pulmonary hypertension was detected in indirect vascular ultrasound.

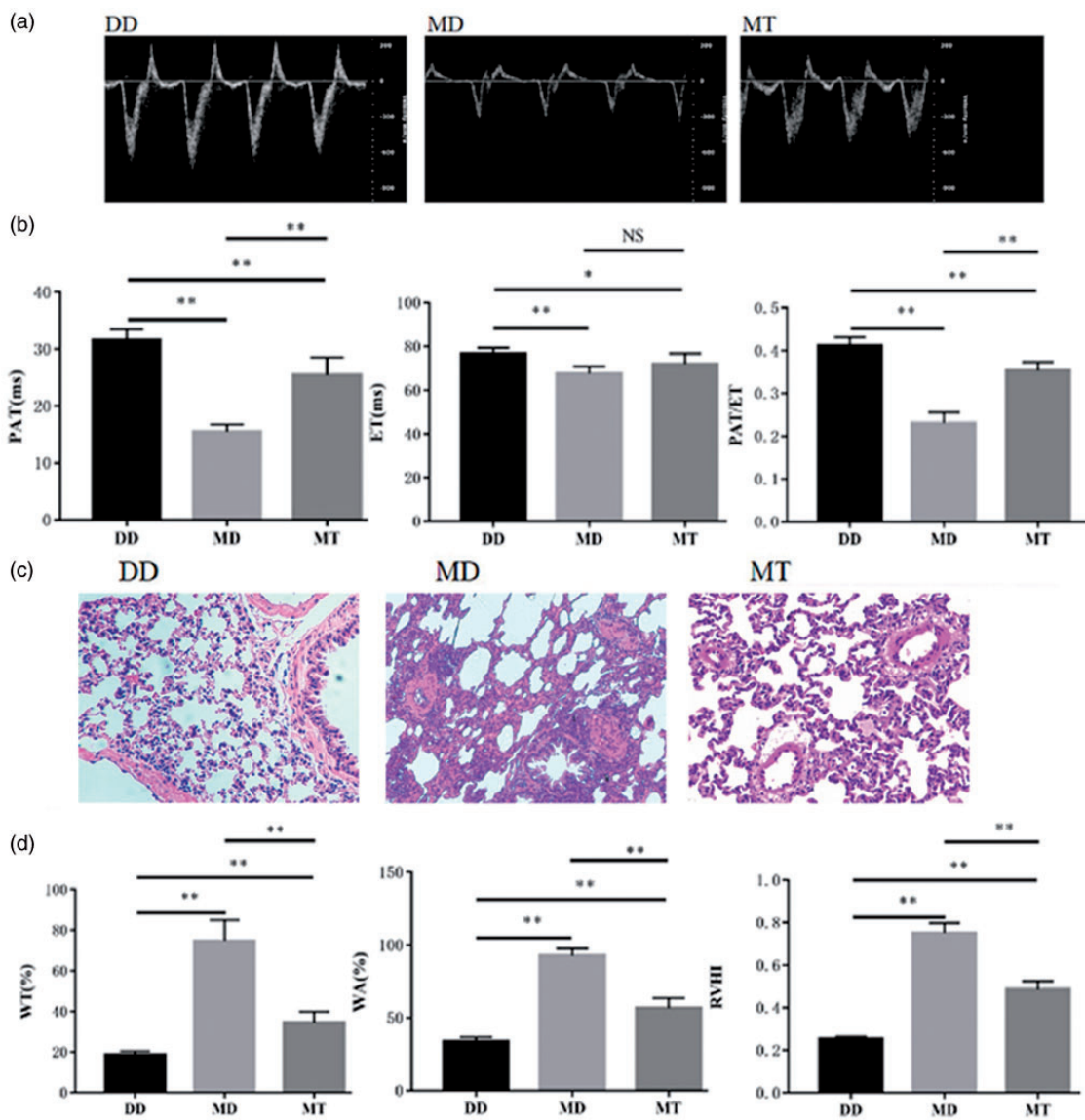


Fig. 4. Effect of TMEM16A_{inh}-A01 on the dynamic outflow of the PA of MCT-treated rats. (a) Representative Doppler images of pulmonary arterial outflow recorded from the negative control rats (DD) that were treated with DMSO to control MCT and then to control TMEM16A_{inh}-A01, the positive control rats (MD) that were treated with MCT for four weeks and DMSO (to control TMEM16A_{inh}-A01), and the rats (MT) treated with MCT for four weeks and then TMEM16A_{inh}-A01. (b) Analytic data for PAT, ET, the PAT/ET ratio. (c) Representative HE-stained slices of pulmonary tissues from normal and MCT-induced PAH rats treated with and without TMEM16A_{inh}-A01. (d) Analytic data for WT%, WA%, the RVHI of normal and MCT-induced PAH rats treated with and without TMEM16A_{inh}-A01. *: P < 0.05 versus control; **: P < 0.01 versus control. n = 6 for each group. DD: DMSO/DMSO; ET: ejection time; MD: MCT/DMSO; MT: MCT/TMEM16A_{inh}-A01; NS: not significant; PAT: pulmonary acceleration time; RVHI: right ventricular hypertrophy index; WT: wall thickness.

The MCT-induced PAH animal model is a classic method of inducing PAH because it is simple to perform.¹⁶ The metabolites derived from MCT in the liver enter the animals' circulatory systems, causing damage to the vascular endothelia and leading to formation of platelet thrombosis in the lung. Consequently, muscularization of non-muscular cells in small vessels is triggered, smooth muscle cells of PAs proliferate, and, eventually, vascular remodeling occurs, followed by the development of PAH. This is not the first description

on effect of MCT, but we still need to explore the pathological and function evolution of MCT-induced PAH model, as the baseline experimental data.

TMEM16A participates in PAH formation

We studied the localization of TMEM16A in vivo, finding that most TMEM16A co-localized with SMA, this was in accordance with results of Forrest et al.'s⁴ study.

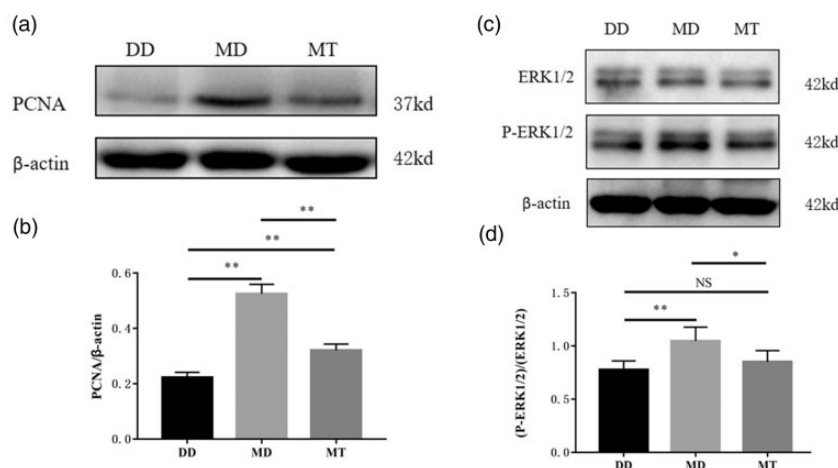


Fig. 5. Effect of T16A_{inh}-A01 on PCNA expression and activation of ERK1/2 in the PAs of MCT-treated rats.

Representative Western blots are shown. (a) Expression of PCNA protein. (b) Analytic data for PCNA protein. (c) Expression and activation of ERK1/2. (d) Analytic data for ERK1/2 and P-ERK1/2. *: $P < 0.05$ versus control; **: $P < 0.01$ versus control. $n = 6$ for each group. DD: ; ERK1/2: MCT/T16A_{inh}-A01; MD: MCT/DMSO; MT: MCT/T16A_{inh}-A01; NS: not significant; PCNA: proliferating cell nuclear antigen.

Table 1. Primer sequences used for RT-qPCR.

Primer sequences		Amplified fragment size (bp)
β-actin (ID: NM_031144)	F:GTGCTATGTTGCCCTAGACTTCG R:GATGCCACAGGATCCATACCC	175 bp ¹⁷
TMEM16 (ID: NM001107564)	F:CCGCAGCGTCCACATCGTGA R:CTGCGGGTCCCCAGGACCAT	240 bp ¹⁸

We speculate that TMEM16A might contribute to PSMCs proliferation. TMEM16A is a promising therapeutic target of PAH. Inhibition/knock-down of TMEM16A reduced the proliferation of PSMCs. Conversely, overexpression of TMEM16A in healthy donor PSMCs produced a PAH-like phenotype.¹⁰ Forrest et al.⁴ conducted a semiquantitative RT-PCR and Western blot analysis, and found TMEM16A overexpression in rats with intraperitoneal injection of MCT for three weeks. We observed that TMEM16A overexpression and pharmacological inhibition of it improved PAH; these results support that TMEM16A overexpression is a harmful factor in the pathogenesis of PAH.

Our studies intended to check the effect on function, not the expression of TMEM16A, so we analyzed mRNA and protein levels of TMEM16A using quantitative RT-PCR and Western blot, and find an expression plateau at four weeks post MCT treatment, as a basis of TMEM16A inhibitor treatment timing. In addition, we choose a TMEM16A inhibitor, which considerably decreased $[Cl^-]$ in the nucleus, exhibited a minimal effect on $[Ca^{2+}]$, and had a negligible effect on TMEM16A at the protein level.¹⁸ PAH and vessel remodeling were still improved by TMEM16A inhibition;

this means that quantitative decrease, or functionally inhibition of TMEM16A, can both reverse vessel remodeling and PAH.

However, there were some contradictory results of the connection between blood pressure and TMEM16A. Vascular-specific overexpression of TMEM16A had no effect on the blood pressure in both basal and Ang II-induced hypertension.¹⁹ Downregulation of TMEM16A expression contributed to the reduction of CaCC in the hypertensive brain basilar artery, and CaCC activity was negatively correlated with blood pressure.²⁰ We speculated this because TMEM16 family members' expression profile and their contributions to the CaCC in vascular smooth muscle cells vary in several types of blood vessels. The expression of TMEM16A-B, TMEM16D-F, and TMEM16K was identified in cultured PSMCs,²¹ and TMEM16A, TMEM16C, TMEM16E, TMEM16F, and TMEM16K are expressed at high level in brain basilar artery.²⁰ Other family members may compensate the effects of TMEM16A on blood pressure and CaCC. Inhibiting one of the family members may even cause a rebound increase in other family members. Specific inhibition of TMEM16A and more detailed exploration of the changes in the expression profiles of other family members caused by it help to make the experimental conclusion clearer.

Inhibition of TMEM16A ameliorate SMC proliferation

TMEM16A was investigated as an anti-cancer target, since it is involved in growth, migration, and invasion of cancer cells, and cell cycles were inhibited from the G1 to S phase in the TMEM16A knockdown experiment.²² In our results, inhibition of TMEM16A reduced the proliferation marker (PCNA) expression, and the results of HE staining showed

that most proliferate cells are SMC in PAH model, suggesting that TMEM16A is probably a pro-proliferating factor for vascular smooth muscle cells. In vitro experiment also reported that TMEM16A inhibition could inhibit the proliferation of SMCs.^{11,19}

T16Ainh-A01 is a promising drug to improve vascular remodeling

Consecutive T16Ainh-A01 administration in PAH rats obviously improve vascular remodeling, even in later stage of PAH, when PA walls thicken and TMEM16A expression was high. T16Ainh-A01 had a negligible effect on TMEM16A at the protein level.¹⁸ We choose the fourth week post MCT treatment to administer T16Ainh-A01, to make sure that T16Ainh-A01 could functionally and not quantitatively inhibit TMEM16A. We consider the improvement of vascular remodeling by T16Ainh-A01 treatment was not dependent on the TMEM16A protein level.

Pharmacological inhibition has poorer selectivity than genetic method. T16Ainh-A01 relax rodent resistance arteries in a concentration dependent way, an equivalent vasorelaxation occurs in rodent arteries when the transmembrane chloride gradient is abolished with an impermeant anion,²³ this reduces the reliability of T16Ainh-A01's dependence on TMEM16A. The comprehensive mechanism needs further research, but the vascular remodeling improvement of T16Ainh-A01 administration is explicit and this makes T16Ainh-A01 as a promising drug in PAH treatment.

ERK1/2 is one of the downstream factors involved in the remodeling effects of TMEM16A

In our present study, pharmacologic TMEM16A inactivation alleviated ERK phosphorylation in PA. ERK1/2 is activated by acute hypertension in vivo.²⁴ The alleviated ERK phosphorylation by T16Ainh-A01 is probably due to its inhibitory effects on PAH and PA remodeling.

The connection between ERK and TMEM16A is contradictory in the previous experiments. TMEM16A activation increased the phosphorylation of ERK1/2, and pharmacologic and genetic inactivation of ERK1/2 abrogated the growth effect of TMEM16A in various cell types.^{14,15} Whereas, in a transgenic mouse that overexpresses TMEM16A, the over activity of non-canonical TGF- β 1/ERK was alleviated in the basilar artery during Ang II-induced hypertension.¹⁹ We speculated the reason is that TMEM16A has indirect relationship with ERK or the cell proliferation effect of TMEM16A was mediated by multi-signaling pathway. TMEM16A was reported to promote vascular remodeling by activating ERK/JNK/Smad indirectly through TGF- β 1 secretion promotion.¹⁹ C-fos phosphorylation could also mediate TMEM16A-induced proliferation of human PSMCs.¹⁰ Thus, the influence of ERK phosphorylation might be counterbalanced by other factors.

Conclusions

TMEM16A mRNA and protein levels are upregulated in MCT-induced PAH models. Functionally, inhibition of TMEM16A by T16Ainh-A01 ameliorated PA remodeling by inhibiting SMC proliferation, possibly by ERK1/2 signaling pathway.

Conflict of Interest

The author(s) declare that there is no conflict of interest.

Ethical approval

The Guide for the Care and Use of Laboratory Animals (the National Institutes of Health, USA) was followed, and the protocols for animal experiments were approved by the Ethics Committee of the Affiliated Hospital, Qingdao University.

Funding

The author(s) disclosed receipt of the following financial support for the research, authorship, and/or publication of this article: This study is supported by National Key R&D Program of China (2016YFC1000808), the National Natural Science Foundation of China (81470926), Shandong Province Natural Science Foundation (ZR2019MH110), and Bureau Science and Technology of Qingdao (16-6-2-16-nsh, 19-6-1-19-nsh).

ORCID iD

Jianye Xie  <https://orcid.org/0000-0002-9103-151X>

References

1. Crosswhite P and Sun Z. Molecular mechanisms of pulmonary arterial remodeling. *Mol Med* 2014; 20: 191–201.
2. Olschewski A, Papp R, Nagaraj C, et al. Ion channels and transporters as therapeutic targets in the pulmonary circulation. *Pharmacol Ther* 2014; 144: 349–368.
3. Caputo A, Caci E, Ferrera L, et al. TMEM16A, a membrane protein associated with calcium-dependent chloride channel activity. *Science* 2008; 322: 590–594.
4. Forrest AS, Joyce TC, Huebner ML, et al. Increased TMEM16A-encoded calcium-activated chloride channel activity is associated with pulmonary hypertension. *Am J Physiol Cell Physiol* 2012; 303: C1229–C1243.
5. Hubner CA, Schroeder BC and Ehmke H. Regulation of vascular tone and arterial blood pressure: role of chloride transport in vascular smooth muscle. *Pflugers Arch* 2015; 467: 605–614.
6. Huang F, Wong X and Jan LY. International Union of Basic and Clinical Pharmacology. LXXXV: calcium-activated chloride channels. *Pharmacol Rev* 2012; 64: 1–15.
7. Wang K, Ma J, Pang Y, et al. Niflumic acid attenuated pulmonary artery tone and vascular structural remodeling of pulmonary arterial hypertension induced by high pulmonary blood flow in vivo. *J Cardiovasc Pharmacol* 2015; 66: 383–391.
8. Zawieja SD, Castorena JA, Gui P, et al. Ano1 mediates pressure-sensitive contraction frequency changes in mouse lymphatic collecting vessels. *J Gen Physiol* 2019; 151: 532–554.
9. Wang B, Li C, Huai R, et al. Overexpression of ANO1/TMEM16A, an arterial Ca²⁺-activated Cl channel, contributes to spontaneous hypertension. *J Mol Cell Cardiol* 2015; 82: 22–32.

10. Papp R, Nagaraj C, Zabini D, et al. Targeting TMEM16A to reverse vasoconstriction and remodelling in idiopathic pulmonary arterial hypertension. *Eur Respir J* 2019; 53(6).
11. Askew Page HR and Dalsgaard T. TMEM16A is implicated in the regulation of coronary flow and is altered in hypertension. *Br J Pharmacol* 2019; 176: 1635–1648.
12. Zeng X, Huang P, Chen M, et al. TMEM16A regulates portal vein smooth muscle cell proliferation in portal hypertension. *Exp Ther Med* 2018; 15: 1062–1068.
13. Jones JE, Mendes L, Rudd MA, et al. Serial noninvasive assessment of progressive pulmonary hypertension in a rat model. *Am J Physiol Heart Circ Physiol* 2002; 283: H364–H371.
14. Duvvuri U, Shiwarski DJ, Xiao D, et al. TMEM16A induces MAPK and contributes directly to tumorigenesis and cancer progression. *Cancer Res* 2012; 72: 3270–3281.
15. Sun M, Sui Y, Li L, et al. Anoctamin 1 calcium-activated chloride channel downregulates estrogen production in mouse ovarian granulosa cells. *Endocrinology* 2014; 155: 2787–2796.
16. Yin J, You S, Liu H, et al. Role of P2X7R in the development and progression of pulmonary hypertension. *Respir Res* 2017; 18: 127.
17. Lérias J, Pinto M, Benedetto R, et al. Compartmentalized crosstalk of CFTR and TMEM16A (ANO1) through EPAC1 and ADCY1. *Cell Signal* 2018; 44: 10–19.
18. Tian XQ, Ma KT, Wang XW, et al. Effects of the calcium-activated chloride channel inhibitors T16Ainh-A01 and CaCCinh-A01 on cardiac fibroblast function. *Cell Physiol Biochem* 2018; 49: 706–716.
19. Zeng XL, Sun L, Zheng HQ, et al. Smooth muscle-specific TMEM16A expression protects against angiotensin II-induced cerebrovascular remodeling via suppressing extracellular matrix deposition. *J Mol Cell Cardiol* 2019; 134: 131–143.
20. Wang M, Yang H, Zheng LY, et al. Downregulation of TMEM16A calcium-activated chloride channel contributes to cerebrovascular remodeling during hypertension by promoting basilar smooth muscle cell proliferation. *Circulation* 2012; 125: 697–707.
21. Manoury B, Tamuleviciute A and Tammaro P. TMEM16A/anoctamin 1 protein mediates calcium-activated chloride currents in pulmonary arterial smooth muscle cells. *J Physiol* 2010; 588: 2305–2314.
22. Sui Y, Sun M, Wu F, et al. Inhibition of TMEM16A expression suppresses growth and invasion in human colorectal cancer cells. *PLoS One* 2014; 9: e115443.
23. Boedtker DM, Kim S, Jensen AB, et al. New selective inhibitors of calcium-activated chloride channels – T16A(inh)-A01, CaCC(inh)-A01 and MONNA – what do they inhibit? *Br J Pharmacol* 2015; 172: 4158–4172.
24. Xu Q, Liu Y, Gorospe M, et al. Acute hypertension activates mitogen-activated protein kinases in arterial wall. *J Clin Invest* 1996; 97: 508–514.